A E690K/E690K

B

C

D W308R/W308R

E

F W308R iPSC   E690K iPSC

TRA 1-81

H

E690K-iPSC 46, XX   cE690-iPSC 46, XX

W308R-iPSC 46, XX   cW308-iPSC 46, XX

G

Exon 9: c.922T>C, p.W308R

PAM

Coding 5' ....TGG AGT GCC CGG TTC.... 3'

3'....ACC TCA CGG GCC AAG.... 5'

Trp Ser Ala Arg Phe

Cas9
gRNA

CGG

ssDNA correction template (70bp)

Donor Constuct/ Post Gene Correction:

AleI

Coding 5' ....TG G AGT GCC TGG TTC.... 3'

3'.....AC C TCA CGG TCC AAG.... 5'

Trp Ser Ala Trp Phe

Homologous recombination

Clone 1 | Clone 2   AleI
- + - +

Sanger seq

Exon 17: c.2068G>A, p.E690K

PAM

Coding 5' ....GAC AAG CCC ACC TCG.... 3'

3'....CTG TTC GGG TGG AGC.... 5'

Asp Lys Pro Thr Ser

Cas9
gRNA

AAG

ssDNA correction template (70bp)

Donor Constuct/ Post Gene Correction:

AatII

Coding 5' ....GAC GAG CCG A CG TC A .... 3'

3'.....CTG CTC GGC T GC AG T .... 5'

Asp Glu Pro Thr Ser

Homologous recombination

Clone 1 | Clone 2   AatII
- + - +

Sanger seq

I

	E690K individual	W308R individual
	36 weeks gestation	Term, C-section
	NRDS	NRDS, ILD
	Treated with CPAP, mechanical ventilation, nitric oxide, furosemide, steroids, surfactant	Treated with CPAP, chronic mechanical ventilation requiring tracheostomy, nitric oxide, steroids, hydroxychloroquine, surfactant
		Recurrent respiratory infections
	Lung transplant at 5 mo	Lung transplant at 21 mo

Figure S1 Clinical records and generation of E690K and W308R ABCA3 mutant patient iPSCs and syngeneic controls

(A) Chest x-ray of patient carrying homozygous E690K ABCA3 mutations showing bilateral pulmonary infiltrates.

(B) H&E staining of lung explant from the patient in panel (A), showing extensive alveolar remodeling, type II cell hyperplasia, interstitial thickening, lymphoid aggregates, and neutrophilic infiltrates. Scale bars, 100µm left, 25µm right. Airway (AW).

(C) TEM images of tissue from (B), showing irregular, small LBs (black arrow heads). Scale bars, 1µm.

(D) Chest x-ray of patient carrying homozygous W308R ABCA3 mutations, showing bilateral pulmonary infiltrates.

(E) H&E staining of explant from patient in (D), showing diffuse type II cell hyperplasia, intraalveolar macrophages, alveolar septal widening with interstitial fibrosis. Scale bars, 50µm left, 25µm right.

(F) TRA 1-81 pluripotency marker immunostains (green) of reprogrammed E690K and W308R iPSC colonies.

(G) CRISPR-Cas9 bi-allelic gene correction strategy for homozygous W308R (top) and E690K (bottom) mutations (red nucleotides). To facilitate screening of corrected clones, silent mutations (blue nucleotides) were introduced in the donor ssDNA correction template; successful homologous recombination was screened using restriction enzyme (AleI, AatII) digest, followed by Sanger sequencing confirmation.

(H) G-banding karyotypes of patient iPSC lines pre- and post- CRISPR-Cas9 gene correction.

(I) Clinical course from birth to lung transplantation in E690K and W308R ABCA3 mutant individual, also see supplemental methods.

NRDS= Neonatal respiratory distress syndrome; ILD= interstitial lung disease.
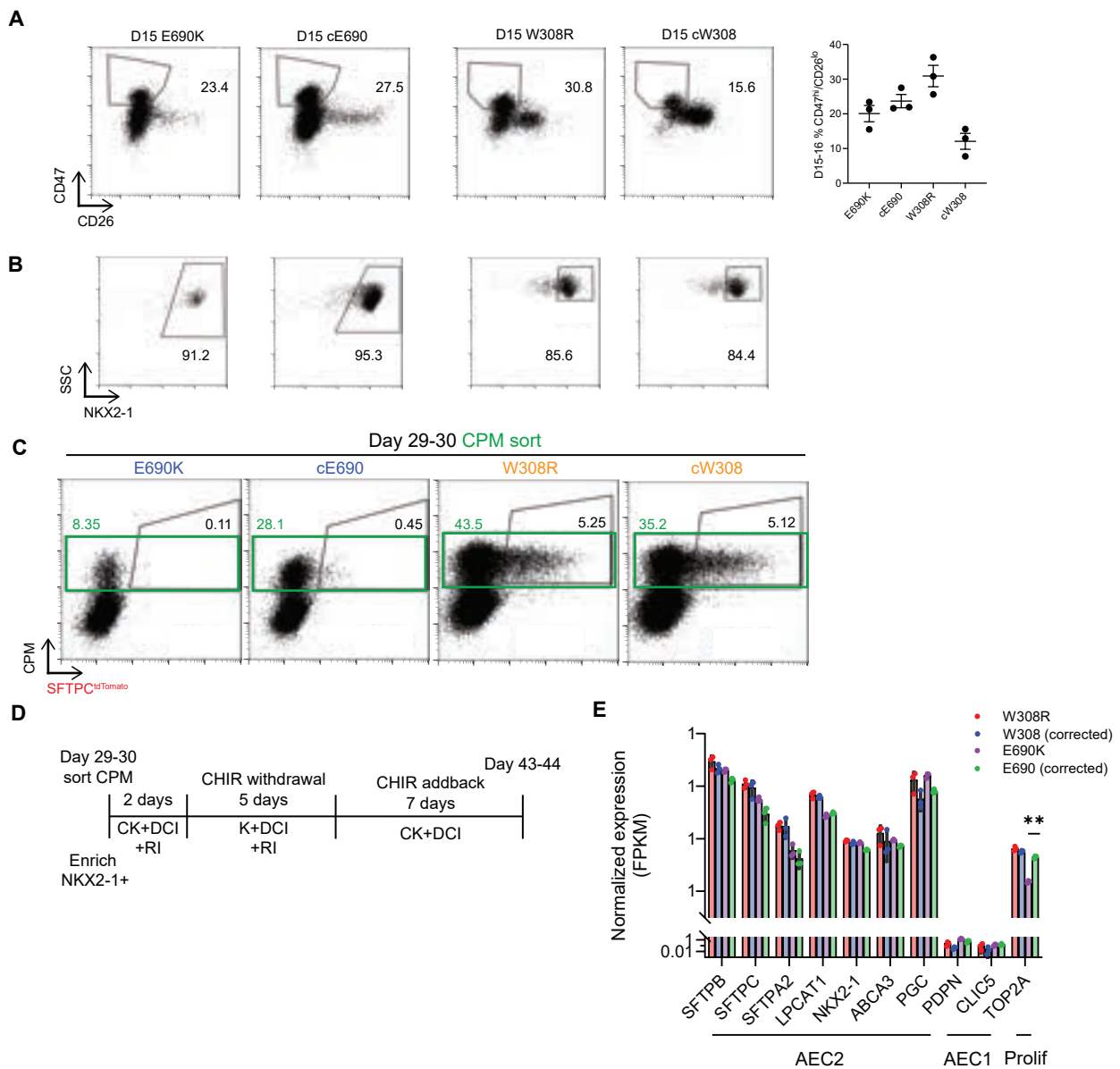
Figure S2 Step-wise directed differentiation and sorting to enrich NKX2-1+ distal lung epithelial progenitor cells during early stages of differentiation of patient-specific iPSCs (see also figure 1).

(A) Representative flow cytometry analyses of day 15 CD47hi/CD26lo cell sorting in all patient lines showing gates used for cell sorting to enrich for NKX2-1 expressing cells, according to methods detailed in Jacob et al. 2019. Biological triplicate separated at day 0, n=3. Bars, mean ± SE.

(B) Representative NKX2-1 intracellular staining analyzed by flow cytometry, showing enrichment of NKX2-1 expressing cells in all patient lines following CD47hi/CD26lo sorting. Dot plots are representative of triplicates samples.

(C) Representative flow cytometry analyses of day 29-30 CPM sorts to enrich for NKX2-1+ distal lung epithelial cells in all patient lines, showing percentages of cells expressing CPM (green gate) and SFTPCtdTomato reporter (black gate).

(D) Timeline of CPM sort and CHIR withdrawal and addback from day 29-30 to day 43-44 of distal lung differentiation to enhance expression of the SFTPCtdTomato reporter.

(E) Graph showing normalized expression of AEC2, AEC1, and proliferative markers in W308R and E690K mutant and corrected iAEC2s. Measured in fragments per kilobase of transcript per million mapped reads (FPKM) from bulk RNA sequencing; n=3. NB: TOP2A is the only significantly differentially expressed transcript shown, comparing mutant to corrected iAEC2s. **FDR adjusted p-value ≤0.01.
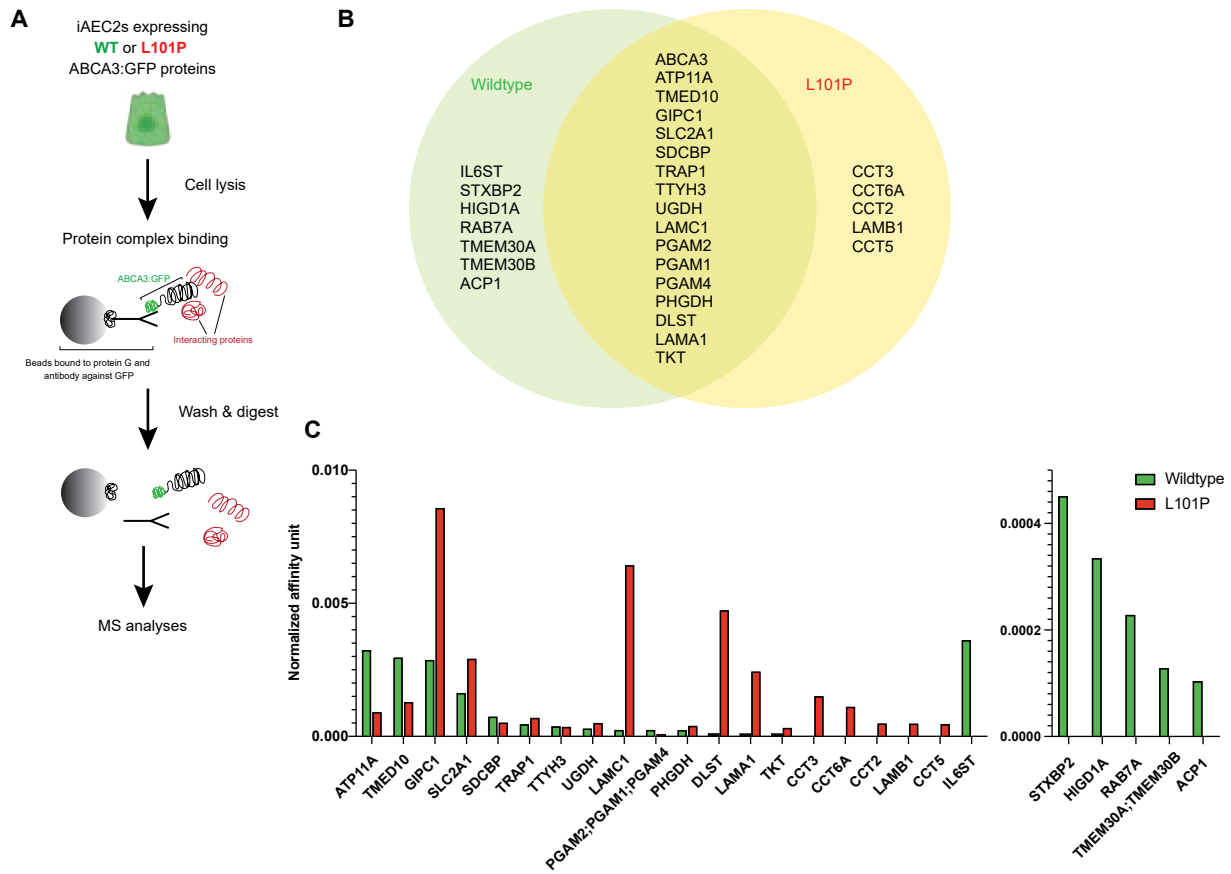
Figure S3 Mass spectrometry analyses of co-immunoprecipitated protein extracts from iAEC2s expressing wildtype or L101P mutant ABCA3:GFP proteins reveal unique, mutant-specific vs wildtype-specific candidate protein-protein interactions
(A) Schematic showing lysis of iAEC2s followed by co-immunoprecipitation (co-IP) followed by mass spectrometry (MS) analyses to identify proteins potentially interacting with wildtype and L101P ABCA3:GFP fusion proteins.
(B) Venn diagram showing proteins identified as potentially interacting with either wildtype or L101P mutant or both ABCA3:GFP fusion proteins.
(C) Bar graph showing affinity unit of shared and genotype-specific interacting protein partners to wildtype or L101P ABCA3:GFP fusion proteins. Normalized to the level of ABCA3 peptides in each co-IP/MS preparation.
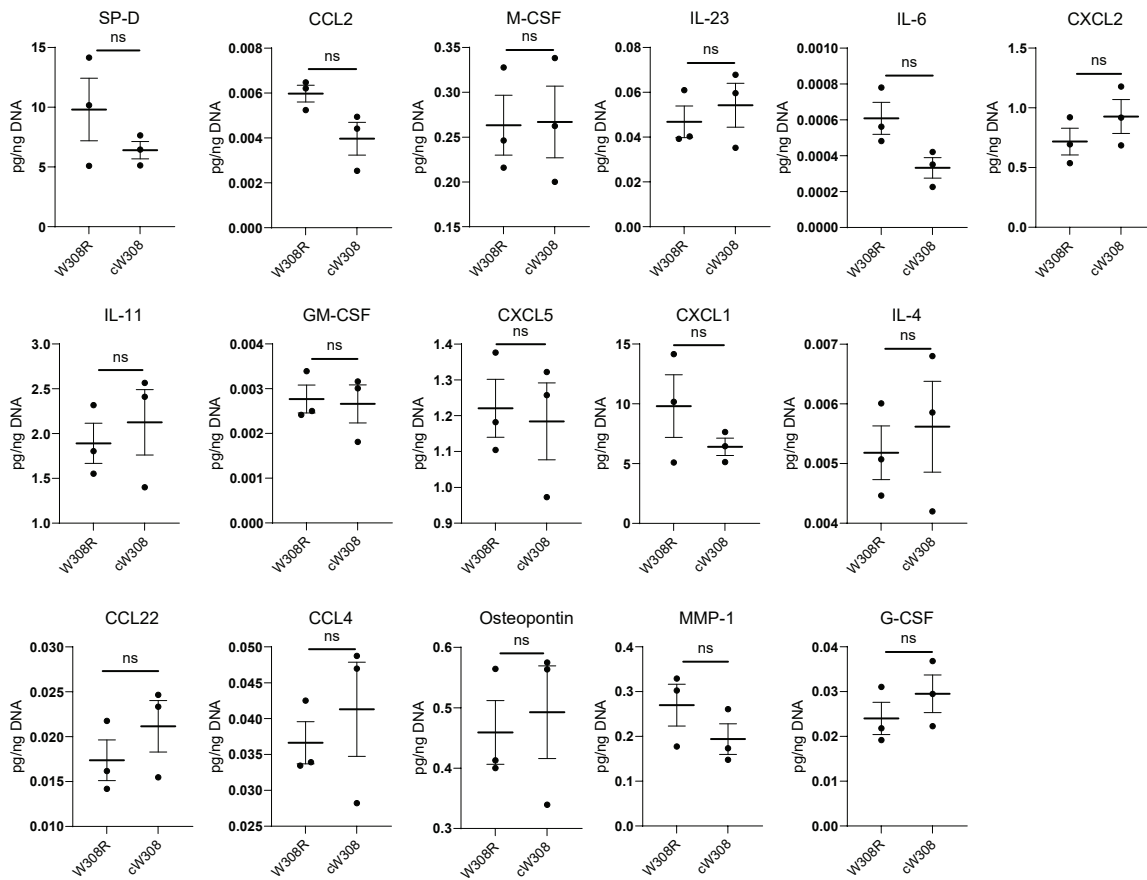
Figure S4 Measurement of cytokines and chemokines in supernatants of patient iAEC2s
Levels of indicated cytokines and chemokines released in the culture supernatants of 2D mono-layer cultured patient iAEC2s homozygous for the W308R mutation compared to corrected (cW308). Biological replicates (n=3), separated at day 0. Bars represent mean ± SE. **p≤ 0.01, two-tailed Student's t-test.
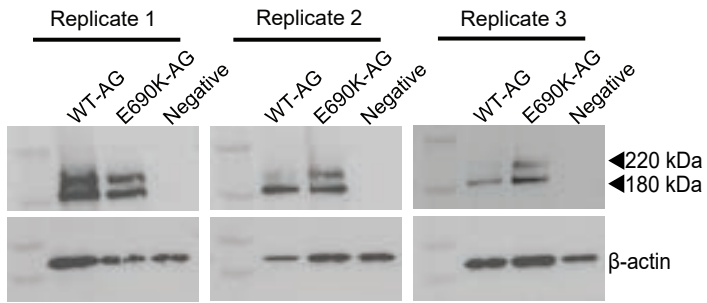
Figure S5 Processing of ABCA3 WT and mutant proteins in human iAEC2s
Western blots using an antibody against GFP to compare protein processing of ABCA3:GFP WT vs. E690K in iAEC2s. Negative controls are iAEC2s without the ABCA3:GFP fusion protein.

SUPPLEMENTAL METHODS:

Clinical, radiographic, and histologic phenotyping of donors with chILD

One patient with homozygous E690K and one patient with homozygous W308R *ABCA3* mutations each presented with rapid onset of neonatal respiratory symptoms which were refractory to all treatments. The patient with homozygous E690K *ABCA3* mutation (c.2068G>A) was a female infant born at 36 weeks gestation. Further genetic analysis revealed her homozygous *ABCA3* mutation to be the result of uniparental disomy of the maternal mutant allele. Within a few hours of birth, the patient developed symptoms of respiratory distress with chest radiographs revealing persistent bilateral pulmonary infiltrates (Fig S1A). An echocardiogram demonstrated tricuspid regurgitation and signs of pulmonary hypertension. Treatment for her respiratory symptoms with mechanical ventilation, supplemental oxygen, nitric oxide, steroids, and multiple doses of exogenous surfactant were ineffective, resulting in persistent respiratory failure. The patient received a bilateral lung transplant at 5 months of age. Explant histology demonstrated diffuse interstitial fibrosis, extensive alveolar remodeling with cystic spaces, diffuse AEC2 hyperplasia, extensive neutrophilic infiltrates of the airways and alveoli, chronic interstitial inflammation with lymphoid aggregates, and intimal thickening of small pulmonary arteries (Fig 1A, S1A, B). Electron microscopy of AEC2s demonstrated small, dense lamellar bodies and tightly wound, small lamellar structures (Fig S1C). Genetic evaluation found no mutations in other genes associated with surfactant production, such as SFTPC or SFTPB genes.

The patient identified with homozygous W308R ABCA3 mutation (c.922T>C) was a term female infant who developed progressive tachypnea, increased work of breathing, and respiratory failure requiring mechanical ventilation. A chest CT taken at 1 month of age demonstrated diffuse, severe, bilateral interstitial infiltrates, ground glass opacities and scattered small cystic areas (Fig S1D). Treatment with exogeneous surfactant, supplemental oxygen, steroids, and hydroxychloroquine, did not result in clear improvement in lung function. Due to persistent respiratory failure and recurrent infections from her underlying lung disease, at 21 months of age the patient underwent lung transplantation. Explant histology demonstrated extensive alveolar remodeling diffuse AEC2 hyperplasia, intra-alveolar macrophages, alveolar septal thickening and interstitial fibrosis (Fig 1A, S1E).

Patient iPSCs and reprogramming and maintenance

All human iPSCs were maintained in feeder free conditions, cultured on Matrigel-coated (Corning, 354277) plates in mTeSR media (StemCell Technologies, 85850), and passaged using Gentle Cell Dissociation Reagent (StemCell Technologies, 100-0485). Reprogramming of the BU3 human iPSC line was previously reported in Kurmann et al. (1) and editing of this line to target an ABCA3:GFP fusion cassette to the endogenous ABCA3 locus (BU3-AG) was previously reported (2). Maintenance, editing, and directed differentiation of these lines was performed under regulatory approval of the Boston University Institutional Review Board (IRB; protocol H-33122) with donor informed consent. For derivation of ABCA3 mutant patient-specific iPSC lines, patient tissue

47 samples were received from Washington University School of Medicine after review and
48 approval by the Human Research Protection Office of Washington University School of
49 Medicine. Genetic evaluation found no mutations in other genes associated with
50 surfactant production, such as SFTPC or SFTPB genes. Reprogramming of dermal
51 fibroblasts from the patient with homozygous E690K *ABAC3* was performed using the
52 excisable floxed STEMCCA lentiviral vector, followed by vector excision with transient
53 Cre transfection as we have previously published (3). Clone "ABCA31" (alias ABCA3
54 SP300) was selected for this project. Dermal fibroblasts from the patient with W308R
55 *ABCA3* was performed with the Sendai virus Cytotune 2 Kit (Thermo Fisher, A16517)
56 according to the manufacturer's instructions. Clone "ABCA35" (alias ABCA3 W308R) was
57 selected for this project. Picked candidate clones from each genotype were characterized
58 for pluripotency by staining for pluripotency markers using monoclonal mouse antibodies
59 against TRA1-81 and TRA 1-60 (Stem Cell Technologies, Catalog # 60065AD.1, Catalog
60 # 60064AD.1) and found to be karyotypically normal (Cell Line Genetics; Figure S1). All
61 iPSC lines produced are catalogued and can be requested through the Center for
62 Regenerative Medicine (CReM) of Boston University and Boston Medical Center, via their
63 iPSC Core and Lung Disease Specific Biorepository: www.crem.bu.edu.
64
65 ***Gene Editing of Human iPSC Lines***
66 E690K and W308R ABCA3 mutant patient-derived iPSC lines were mono-allelically
67 targeted with a tdTomato reporter at the ATG of the endogenous SFTPC locus using
68 TALENS gene editing tools following the same methods detailed in Jacob et al. (4).
69
70 <u>CRISPR-Cas9 gene editing of the ABCA3 locus to correct or knock-in mutations:</u>
71 For bi-allelic, foot-print free ABCA3 gene correction of patient iPSC lines, a 20bp guide
72 RNA (gRNA) specific to either the E690K mutation 5'-GATGGCGTCCATGCCCGAGG-3'
73 or the W308R mutation 5'-GCTGGCTGCACTGGAGTGCCCGG-3' was designed using
74 crispr.mit.edu, based on proximity to mutation site and fidelity score. Each gRNA was
75 inserted using conventional cloning techniques into pSpCas9 plasmids (5) containing
76 sequences encoding the Cas9 protein and GFP. For homologous recombination after
77 CRISPR Cas9-induced double stranded break, 70 bp single stranded DNA
78 oligonucleotide (ssODN) donors were designed for gene-correction for the E690K
79 mutation (5' ACTGTGTCTCTCCCTCCAGGTGCTGATACTGGAC GAG CCG ACG TCA
80 GGC ATG GAC GCC AT C TCCAGGAGG 3') and the W308R mutation (5'
81 GGCGATGAGGAGGAAGAGGAAGAACAAGAGGAACCAAGCGCTCCAGTGCAGCCA
82 GCTGCTGAGCCCCATC 3'). Each donor ssODN contains silent mutations resulting in
83 DNA sequences recognized by restriction enzymes (AatII site for E690K, and AleI for
84 W308R) upon successful homologous recombination, allowing for screening of iPSC
85 clones with restriction digestion of PCR products.
86
87 iPSC nucleofection of plasmids and ssODNs was performed using the P3 Primary Cell
88 4D-Nucleofector X Kit (Lonza, cat no. V4XP-3024). $5X10^6$ iPSCs were nucleofected with
89 5μg of pSpCas9 plasmid containing desired gRNA and 5μg of ssODN in 100 μl total
90 volume of P3 nucleofection solution (Lonza) and re-plated on 4 wells of matrigel coated
91 6-well tissue culture dish (Corning), fed with mTeSR media (Stem Cell Technologies) and
92 rock inhibitor (RI), then re-fed with just mTeSR after 24 hours. 48 hours after nucleofection,

93   GFP+ cells were sorted and plated at a density of 1,000-3,000 cells per well of a 6 well
94   tissue culture plated pre-seeded with mouse embryonic fibroblast (MEF) feeder cells.
95   After approximately 2 weeks, clonal outgrowths were harvested for genomic DNA for PCR
96   screening using primer pairs designed to surround the region of homologous
97   recombination,   F: 5'   AAGGGCCTGTCACGTCAGAA   3',   R: 5'
98   CTGATCTGAGGGCCCTTCATGAA 3' for the E690K locus, and primer pairs, F: 5'
99   CAGGCGCTTTTGGTCAGTGAA 3', R: 5' CTACATTTGGCTTCACCTGCAGG 3', for the
100   W308R locus. PCR amplicons were screened using restriction enzyme digestion as
101   shown in the supplemental figures. Gene-correction of successfully digested clones was
102   confirmed by Sanger sequencing.
103
104   For CRISPR Cas9 single nucleotide E690K and W308R mutagenesis of the wildtype
105   BU3$^{ABCA3:GFP}$ iPSC line, the same guide RNAs used for gene-correction of patient-specific
106   iPSC   lines   were   used   in   conjunction   with   new   ssODN   donors: 5'
107   ACTGTGTCTCTCCCTCCAGGTGCTGATACTGGACAAGCCCACCTCGGGCATGGAC
108   GCCATCTCCAGGAGG   3'   for   E690K   mutation,   and   5'
109   GGCGATGAGGAGGAAGAGGAAGAACAAGAGGAACCGAGCGCTCCAGTGCAGCCA
110   GCTGCTGAGCCCCATC 3' for W308R mutation containing mutated sequences.
111
112   For   the   L101P   mutagenesis   of   BU3$^{ABCA3:GFP}$ iPSC   line,   guide   RNA   5'
113   CGTCACTGAGACAGTGCGCAGGG   3'   and   ssODN   of   5'
114   TGTCTCACCTCGCATGTTGATCACAGGTGCTCTGCGCACTGTCTCAGTGACGGTCT
115   TGGCAGCGTCACTG 3' was used, containing restriction digest sequence for BsiHKAI
116   restriction enzyme for recombination screening of targeted clones.
117
118   ***Directed Differentiation and Maintenance of iAEC2s***
119   Directed differentiation of iAEC2s were performed as detailed in our previously published
120   protocol (4, 6). In brief, day 0 PSCs were differentiated into definitive endoderm (day 0-3)
121   using StemDiff Endoderm Kit (Stem Cell Technologies, 05110), followed by anterior
122   foregut endoderm (day 3-6) using DS/SB media (2uM dorsomorphin, Stemgent, 040024;
123   10μM SB431543, Biotechne, 1614), then further specified into NKX2-1+ lung epithelial
124   progenitors using CBRa media (3μM CHIR99021, Biotechne, 4423; 10ng/ml rhBMP4,
125   BioTechne, 314BP; 100nM retinoic acid, Sigma-Aldrich, R2625; day 6-15). On day 15,
126   NKX2-1 expressing lung epithelial progenitors were sorted either by NKX2-1^{GFP}(BU3-
127   NGST line) or using CD47^{hi}/CD26^{lo} sorting to enrich for NKX2-1+ cells (7). Sorted cells
128   were plated in 3D Matrigel cultures and fed with distalizing CK+DCI media (3μM
129   CHIR99021, 10ng/ml KGF, 50nM dexamethasone, 0.1mM cyclic AMP and 0.1mM IBMX),
130   as detailed in Jacob et al. (6).
131
132   Additionally, to increase the frequencies of SFTPC^{tdTomato} or ABCA3:GFP-expressing
133   iAEC2s, CHIR "withdrawal and addback" to distal lung progenitor cells was conducted as
134   previously published in Jacob et al. (6), first by plating day 30 CPM sorted cells in 3D
135   matrigel and feeding with CK+DCI and RI for 48 hours, followed by re-feeding with KGF+
136   DCI and RI (KDCI+RI; i.e. "CHIR withdrawal") for 5 days, followed by re-feeding with the
137   standard CK+DCI media for the duration of the experiment indicated in the text..
138

139 ***2D Monolayer Culture of iAEC2s***
140 2D monolayered iAEC2 culture were made by plating either day 15 CD47hi/CD26lo
141 sorted lung progenitors, or day 43+ alveolospheres, after treating with trypsin to prepare
142 a single-cell suspension. Single cell suspensions were then plated on Matrigel-coated 48-
143 well tissue culture plates (Corning) at 300,000 to 600,000 cells per well. 2D cultures were
144 fed with CK+DCI with RI every other day until confluent.
145
146 **Quantification of intracellular vesicle/lamellar body size by ABCA3:GFP**
147 **fluorescence microscopy**
148 For measurements of ABCA3:GFP+ vesicles in wildtype and *ABCA3* mutant iAEC2s, 50
149 representative vesicles were measured using ImageJ software measuring tool across
150 three separate images per genotype and across 8-10 cells. Measurement of A549 cells
151 expressing wildtype or mutant ABCA3:GFP+ vesicles was performed on confocal
152 microscopy images using the NIS-Elements software (Nikon).
153
154 ***Quantitative RT-qPCR***
155 qRT-PCR measuring expression levels of key AEC2 and non-lung endodermal genes
156 was performed as we detailed previously in Hawkins et al. (7). Briefly, RNA was harvested
157 following the manufacturer's instructions using Qiazol and miRNeasy mini kits (QIAGEN).
158 cDNA was generated by reverse transcription of 100ng RNA from each sample using
159 Applied Biosystems High-Capacity cDNA Reverse Transcription Kit. For qPCR, either
160 20μl reactions (for use in Applied Biosystems StepOne 96-well System) or 12 μl reactions
161 (for use in Applied Biosystems QuantStudio7 384-well System) were prepared using 2μl
162 of diluted cDNA and run for 40 cycles. All primers were TaqMan probes from Applied
163 Biosystems (specific primer cat. no. referenced in Jacob et al. (4)). Relative expression
164 was calculated using average cycle value (Ct) of samples normalized to 18S control and
165 reported as fold change ($2^{-\Delta\Delta Ct}$), with fold change of 1 assigned to day 0 undifferentiated
166 PSCs, unless otherwise indicated in the text. For genes that were undetectable after 40
167 cycles of PCR, a Ct value=40 was assigned to allow fold change calculations.
168
169 ***Surfactant secretion after secretagogue stimulation of iAEC2s as measured by***
170 ***fluorescence microscopy and mass spectrometry***
171 For visualization of phospholipid secretion using day 75 BU-AG iAEC2s, day 72 cultured
172 ABCA3:GFP+ iAEC2s were single-cell dissociated and plated as a 2D monolayer on
173 Matrigel-coated coverslip-bottomed dishes (MatTek, part no. P35G-1.5-14-C) at 1×10^6
174 cells per well. iAEC2 secretion was induced using a secretagogue cocktail consisting of
175 final concentrations of 100nM ATP (Thermo Fisher cat no. R0441) and 300nM Phorbol12-
176 myristate 13-acetate (PMA, Cayman Chemicals, item no. 10008014). Visualization of
177 secreted lipid contents was achieved by feeding cultured cells with 5μg/mL of FM4-64
178 dye (Thermo Fisher, cat no. T13320) 20 min prior to induction with or without
179 secretagogues.
180
181 For lipidomic analyses of patient iAEC2 supernatants, day 171-173 patient iAEC2s from
182 triplicate differentiations (n=3, separated from day 0 on for E690K vs cE690 syngeneic
183 pairs) and separated at day 133 on (for W308R vs cW308 syngeneic pairs) were plated
184 in 2D monolayer cultures at 300,000 cells per well and fed with CK+DCI+RI for 14 days.

185 On day 185-187, cells were treated either with the indicated secretagogues or DMSO
186 vehicle control for 24 hours followed by collection of cell pellets for DNA quantitation and
187 culture supernatants for lipidomic analyses by mass spectrometry as detailed in Jacob et
188 al. (4). Total phosphatidylcholine (PC) composition and 32:0 PC
189 (dipalmitoylphosphatidylcholine; DPPC) composition was reported as "Absolute
190 Quantitation" nmol/μg protein or nmol/μg DNA.
191
192 ***Immunofluorescence Imaging***
193 Routine live-cell fluorescence imaging was done using a Keyence BZ-X800 microscope
194 (Keyence, Japan). Live-cell confocal imaging of secretagogue-induced iAEC2 secretion
195 and other 2D plated iAEC2s was conducted using reagents described above and an LSM
196 880 Laser Scanning Confocal Microscope (Zeiss, Germany).
197
198 ***Flow Cytometry and Cell sorting***
199 Preparation of single-cell suspension for flow cytometry and cell sorting was described
200 previously (4, 6). Prepared samples were either directly sorted based on fluorescence
201 reporter expression (ABCA3:GFP, SFTPC[tdTomato], both, or neither) on a MoFlo Astrios
202 Cell Sorter (Beckman Coulter) or stained with primary and secondary antibodies as
203 indicated in the text prior to cell sorting. For day 15 enrichment of NKX2-1+ primordial
204 lung progenitors, cell surface antigen staining for CD47^{hi}/CD26^{lo} cell population was
205 performed using methods previously published in Hawkins et al. (7). For day 30 re-
206 enrichment of NKX2-1+ lung epithelial population, staining of cells in single-cell
207 suspension for CPM for flow cytometry and cell sorting were done at 4°C using primary
208 mouse monoclonal antibodies against human CPM (1:200, Fujifilm Wako, 014-27501) for
209 30min followed by staining with secondary Alexa Fluor 647 conjugated antibody (1:500,
210 ThermoFisher Scientific, A32787) for another 20 min.
211
212
213 ***ABCA3:GFP Co-immunoprecipitation and Mass Spectrometry analyses***
214 To identify potential protein binding partners for ABCA3, we prepared iAEC2 cell pellets
215 as indicated in the text. These pellets were lysed in buffer containing 30 mM Tris-HCl,
216 150 mM NaCl, 1% N-dodecylmaltoside, and complete protease and phosphatase
217 inhibitors (Roche) followed by 1 freeze thaw cycle and sonication at 10%, 15s, 3s pulse.
218 Supernatants were collected after centrifugation at 14,000g for 30 min at 4°C.
219 Immunoprecipitation was performed with anti-GFP (Invitrogen GF28R) or IgG control and
220 Protein G Dynabeads (Invitrogen), 3 hour incubation at 4°C. Protein complex bound
221 beads were washed twice using Lysis buffer without detergent and once with 100 mM
222 triethylammonium bicarbonate. On bead Trypsin digestion was performed with 750ng of
223 trypsin (Pierce) in 100 mM triethylammonium bicarbonate overnight at 37°C. Peptides
224 were desalted using a C18 ZipTip (Millipore) and subjected to reverse-phase LC
225 separation on a 60-min gradient and analyzed on a Q Exactive HF-X (Thermo Fisher
226 Scientific). Data-dependent fragmentation used collision-induced dissociation. RAW files
227 were searched using MaxQuant under standard settings using the UniProt human
228 database, allowing for two missed trypsin cleavage sites, variable modifications for N-
229 terminal acetylation, and methionine oxidation. Candidate peptides and protein
230 identifications were filtered on the basis of a 1% false discovery rate threshold based on

231 searching of the reverse sequence database. To remove potential contaminants, we
232 eliminated proteins detected in IgG control group. Comparison and analyses of potential
233 protein interacting partners between wildtype and L101P ABCA3:GFP mutant fusion
234 protein were performed by normalizing the intensity level of ABCA3 peptides within each
235 of the wildtype and L101P precipitate samples.
236
237 ***Bulk RNA sequencing***
238 The following samples were harvested in Qiazol (QIAGEN) for bulk RNA-sequencing
239 analysis: (1) day 43 SFTPC^{tdTomato}+ E690K patient iAEC2; (2) day 43 SFTPC^{tdTomato}+
240 cE690 patient iAEC2; (3) day 44 SFTPC^{tdTomato}+ W308R patient iAEC2s; (4) day 44
241 SFTPC^{tdTomato}+ cW308 patient iAEC2s; (5) day 43 ABCA3:GFP+ wildtype BU3 iAEC2s;
242 (6) day 44 E690K ABCA3:GFP+ BU3 iAEC2s; (7) day 44 W308R ABCA3:GFP+ BU3
243 iAEC2s. Triplicate differentiations of each line were performed (n=3; separated from day
244 0). RNA extractions, library preparations, and bioinformatic analyses were performed
245 using methods we have previously published (2). The triplicated mutant vs normal control
246 differentiations were prepared and sequenced head-to-head to avoid any potential
247 technical batch artifacts. Briefly, sequencing libraries were prepared from total RNA
248 extracted from each indicated sample using Illumina TruSeq RNA Sample Preparation
249 Kit v2. mRNA was isolated using magnetic bead-based poly(A) selection, fragmented,
250 and randomly fragmented for reverse transcription, followed by synthesis of cDNA
251 fragments. cDNA fragments were then end-paired and ligated to Illumina Paired-End
252 sequencing adapters. The products were end-paired and PCR-amplified to create the
253 final cDNA library. Libraries were sequenced on an Illumina NextSeq 500 to generate an
254 average of 49 million paired-end reads per sample for the patient-specific samples. The
255 sequencing of the 3 libraries from BU3 iPSC-derived iAEC2s generated an average of 53
256 million paired-end reads per sample. The quality of the raw data was assessed using
257 FastQC v.0.11.7. Sequence reads were aligned to a combination of the human genome
258 reference (GRCh38) and GFP reporter sequence, using STAR v.2.5.2b (8). Counts per
259 gene were summarized using the featureCounts function from the subread package
260 v.1.6.2. The edgeR package v.3.25.10 was used to import, organize, filter and normalize
261 the data. Genes that were not expressed in at least one of the experimental groups were
262 filtered out (keeping only genes that had at least 0.5 counts per million of mapped reads
263 in at least 3 libraries). The TMM method was used for normalization. Principal Component
264 Analysis (PCA) and Multidimensional Scaling (MDS) were used for exploratory analysis
265 and to assess sample similarities. Differentially expressed genes (DEGs) between
266 samples were identified by using the limma package v.3.52.0 and its voom method for
267 fitting linear models, doing empirical Bayes moderation to estimate gene-wise variability,
268 and finally, testing significance based on the moderated t-statistic. All DEGs, false
269 discovery rate (FDR)-adjusted p values, and gene expression fold change values are
270 listed in the supplemental tables (tables S1A, S1B, and S2). Gene set analysis was
271 performed using the GSEA package (9). All sequencing datasets have been deposited
272 with the online Gene Expression Omnibus (see main methods section for accession
273 numbers).
274
275 ***EdU incorporation and colony forming efficiency assays***

For colony formation efficiency (CFE) assays, triplicate differentiations (n=3, separated at day 0) of patient ABCA3 mutant or gene-corrected day 43 SFTPC^{tdTomato}-sorted iAEC2s were plated at 400 cells/μl in 25μl 3D matrigel droplet. Stitched, and full focused, Z-stacked bright field images were taken 10 days after cell plating using BZ-X800 Keyence microscope for CFE analyses reported as total number of colonies divided by input cell per droplet. For EdU incorporation assay of SFTPC^{tdTomato}+ iAEC2s, the same cells used for CFE quantitation were inoculated on day 10 with 10μM EdU for 24 hours followed by cell sorting for SFTPCtdTomato+ iAEC2s. Sorted cells were fixed, permeabilized, and stained with the Click-iT reaction mixture (Invitrogen) according to the manufacturer's protocol. The percentage of iAEC2s that incorporated EdU was determined by flow cytometry (Stratedigm, CA, USA).

Measurement of NFκB Pathway Activity in Patient iAEC2s

Bioluminescence quantification of p50/65 heterodimer binding activity was performed in AEC2s using our published lentiviral NFkB signaling reporter vector (10) with methods for transduction of iAEC2s, sorting, and bioluminescence measurements detailed in our prior publication (11). Briefly, day 258 W308R and cW308 patient iAEC2s, and day 158 E690K and cE690 iAEC2s grown in 3D culture were dissociated to single-cell suspension for lentiviral infection. 100,000 iAEC2s from each genotype were infected with the lentivirus at 20 MOI and polybrene for 4 hours at 37 ^{o}C in 1.5ml tube and, plated in triplicate 3D matrigel droplets and re-fed with CK+DCI. 14 days after plating, 15,000 GFP+ infected cells and uninfected cells per genotype were added to 96-well microplates (Thermo Fisher cat. no. M33089) for luminescence measurements using Dual-Luciferase Reporter Assay Kit (Promega) according to manufacturer's recommendations and using Infinite 200 PRO microplate reader (TECAN, Switzerland).

iAEC2 Supernatant Cytokine and Chemokine Measurements

Patient iAEC2 supernatants were collected from triplicate differentiations (all lines separated at day 0, n=3) of day 97 E690K and cE690 patient iAEC2s and day 100 W308R and cW308 patient iAEC2s grown in 2D monolayered culture 8 days after 2D plating on matrigel coated 48-well plates. Supernatant protein concentrations of SP-D, M-CSF, IL-23, GM-CSF, CXCL5, CXCL1, CXCL17, CCL20, CCL11, CCL17, CCL22, CCL4, OPN, MMP-1, MMP7, MMP-10, MMP-13, IL-8, IL-1beta, TNF-alpha, IL-11, IL-13, IL-33, IL-6, IL-4, G-CSF, CXCL1, CXCL2, CX3CL1, CCL2, IFN-alpha, IFN-gamma, IFN-beta, were measured by using human magnetic Luminex assay (R&D systems) on Bio-Plex 200 multiplexing analyzer system (Bio-Rad).

1.   Kurmann AA, Serra M, Hawkins F, Rankin SA, Mori M, Astapova I, et al. Regeneration of Thyroid Function by Transplantation of Differentiated Pluripotent Stem Cells. *Cell Stem Cell.* 2015;17(5):527-42.
2.   Sun YL, Hurley K, Villacorta-Martin C, Huang J, Hinds A, Gopalan K, et al. Heterogeneity in Human Induced Pluripotent Stem Cell-derived Alveolar Epithelial Type II Cells Revealed with ABCA3/SFTPC Reporters. *Am J Respir Cell Mol Biol.* 2021;65(4):442-60.

322 3.   Somers A, Jean JC, Sommer CA, Omari A, Ford CC, Mills JA, et al. Generation
323   of transgene-free lung disease-specific human induced pluripotent stem cells
324   using a single excisable lentiviral stem cell cassette. *Stem Cells.*
325   2010;28(10):1728-40.
326 4.   Jacob A, Morley M, Hawkins F, McCauley KB, Jean JC, Heins H, et al.
327   Differentiation of Human Pluripotent Stem Cells into Functional Lung Alveolar
328   Epithelial Cells. *Cell Stem Cell.* 2017;21(4):472-88 e10.
329 5.   Ran FA, Hsu PD, Wright J, Agarwala V, Scott DA, and Zhang F. Genome
330   engineering using the CRISPR-Cas9 system. *Nat Protoc.* 2013;8(11):2281-308.
331 6.   Jacob A, Vedaie M, Roberts DA, Thomas DC, Villacorta-Martin C, Alysandratos
332   KD, et al. Derivation of self-renewing lung alveolar epithelial type II cells from
333   human pluripotent stem cells. *Nat Protoc.* 2019;14(12):3303-32.
334 7.   Hawkins F, Kramer P, Jacob A, Driver I, Thomas DC, McCauley KB, et al.
335   Prospective isolation of NKX2-1-expressing human lung progenitors derived from
336   pluripotent stem cells. *J Clin Invest.* 2017;127(6):2277-94.
337 8.   Dobin A, Davis CA, Schlesinger F, Drenkow J, Zaleski C, Jha S, et al. STAR:
338   ultrafast universal RNA-seq aligner. *Bioinformatics.* 2013;29(1):15-21.
339 9.   Subramanian A, Tamayo P, Mootha VK, Mukherjee S, Ebert BL, Gillette MA, et
340   al. Gene set enrichment analysis: a knowledge-based approach for interpreting
341   genome-wide expression profiles. *Proc Natl Acad Sci U S A.*
342   2005;102(43):15545-50.
343 10. Wilson AA, Kwok LW, Porter EL, Payne JG, McElroy GS, Ohle SJ, et al.
344   Lentiviral delivery of RNAi for in vivo lineage-specific modulation of gene
345   expression in mouse lung macrophages. *Mol Ther.* 2013;21(4):825-33.
346 11. Alysandratos KD, Russo SJ, Petcherski A, Taddeo EP, Acin-Perez R, Villacorta-
347   Martin C, et al. Patient-specific iPSCs carrying an SFTPC mutation reveal the
348   intrinsic alveolar epithelial dysfunction at the inception of interstitial lung disease.
349   *Cell Rep.* 2021;36(9):109636.
350